Nondipole effects in the angular distribution of photoelectrons from the C K shell of the CO molecule

K. Hosaka,[1] J. Adachi,[1,2] A. V. Golovin,[2,3] M. Takahashi,[4] T. Teramoto,[1] N. Watanabe,[4] T. Jahnke,[5] Th. Weber,[5] M. Schöffler,[5] L. Schmidt,[5] T. Osipov,[6] O. Jagutzki,[5] A. L. Landers,[7] M. H. Prior,[6] H. Schmidt-Böcking,[5] R. Dörner,[5] A. Yagishita,[1,2] S. K. Semenov,[8] and N. A. Cherepkov[8]

[1]*Department of Chemistry, Graduate School of Science, The University of Tokyo, Bunkyo-ku, Tokyo 113-0033, Japan*
[2]*Photon Factory, Institute of Materials Structure Science, Tsukuba-shi, Ibaraki 305-0801, Japan*
[3]*Institute of Physics, St.Petersburg State University, 198504 St.Petersburg, Russia*
[4]*Institute of Multidisciplinary Research for Advanced Materials, Tohoku University, Sendai, Miyagi 980-8577, Japan*
[5]*Institut für Kernphysik, University of Frankfurt, Max-von-Laue-Str 1, 60348 Frankfurt, Germany*
[6]*Lawrence Berkeley National Laboratory, Berkeley, California 94720, USA*
[7]*Physics Department, Auburn University, Auburn, Alabama 36849, USA*
[8]*State University of Aerospace Instrumentation, 190000 St.Petersburg, Russia*

Measurements and calculations of a contribution of the nondipole terms in the angular distribution of photoelectrons from the C K shell of randomly oriented CO molecules are reported. In two sets of measurements, the angular distribution in the plane containing the photon polarization and the photon momentum vectors of linearly polarized radiation and the full three-dimensional photoelectron momentum distribution after absorption of circularly polarized light have been measured. Calculations have been performed in the relaxed core Hartree-Fock approximation with a fractional charge. Both theory and experiment show that the nondipole terms are very small in the photon energy region from the ionization threshold of the K shell up to about 70 eV above it.

I. INTRODUCTION

The electric dipole approximation for a long time was implied to be sufficient for an adequate description of atomic and molecular photoionization in the photon energy region below 1 keV. Only very recent studies, to the best of our knowledge, have revealed the pronounced effects of nondipole contributions on the angular distribution of photoelectrons at these energies. Earlier it was commonly accepted that at low photon energies in the expansion of the electromagnetic wave, $\exp(i\mathbf{k} \cdot \mathbf{r}) = 1 + i\mathbf{k} \cdot \mathbf{r} + \cdots$, one can retain only the first term independent of the photon momentum $\mathbf{k}$, which corresponds to the electric dipole approximation. At higher photon energies the contribution of the next term linear in $\mathbf{k}$ must be included which contains the electric quadrupole and magnetic dipole corrections to the electric dipole approximation. While within the electric dipole approximation the photoelectron angular distributions are rotationally symmetric around the polarization direction, the next term induces a forward-backward asymmetry with respect to the photon propagation. The first observation of such a deviation from the dipole approximation in the angle-resolved photoemission from the Ne atom at relatively low photon energy (about 1250 eV) were reported by Krause [1] and Wuilleumier and Krause [2]. But the systematic studies of nondipole effects started only about ten years ago, owing to the appearance of brilliant synchrotron radiation sources of variable frequency (see [3], and references therein). The theory of nondipole effects in atoms is now fairly well established [4–8]. Under conditions at which the first-order correction to the electric dipole approximation is sufficient (e.g., photon energies be-

low several keV), the main contribution is given by the terms linear in $\mathbf{k}$, that is by the interference between the electric dipole and electric quadrupole plus magnetic dipole terms.

Several reasons have been mentioned for the enlarged contribution of nondipole effects at low photon energies. One of them is the presence of a Cooper minimum in the cross section where the dipole matrix element is approaching zero. Then the relative contribution of the interference between the electric dipole and electric quadrupole or magnetic dipole terms increases [7,8]. The other reason is a resonance in the quadrupole channel which leads to a sharp increase of the quadrupole matrix element. It could be an autoionization resonance [9,10] or a shape resonance [11,12]. While autoionization resonances are usually relatively narrow, shape resonances could be both strong and broad. In particular, a broad shape resonance has been discovered in the quadrupole $np \rightarrow \varepsilon f$ transitions in atoms [12,13] which can lead to a great increase of nondipole effects at photon energies of the order of 100 eV. And finally, due to an interchannel coupling the shape resonance in one channel can induce an increase of a matrix element, and as a consequence an increase of nondipole effects in those channels where the shape resonance does not exist [11]. A joint action of several mechanisms is also possible. As an example, we can mention a large nondipole effect in the photoionization of the Xe $5s$ shell at about 150 eV photon energy predicted theoretically in [11] and observed recently in [14,15]. The effect appears as a result of a joint action of all three different mechanisms mentioned above. The main contribution comes from the minimum in the $5s$ cross section which is the result of a strong interchannel coupling between the $5s \rightarrow \varepsilon p$ and $4d \rightarrow \varepsilon f$ transitions.

The latter has a well-known giant dipole resonance in that energy region. The other contribution comes from the quadrupole shape resonance in the $4p$ shell ($4p \rightarrow \varepsilon f$ transition), which influences the $5s$ shell again through the interchannel coupling.

The studies of nondipole effects in molecules are only starting. The first observation of nondipole effects in the angular distribution of photoelectrons from the K shell of randomly oriented N_2 molecules was reported in [16,17]. A strong maximum in the photon energy dependence of nondipole parameter $\zeta = \gamma + 3\delta$ [see Eq. (1) below] has been observed at about 50 eV above the K shell ionization threshold. The position of this resonancelike structure does not coincide with the well-known σ^* shape resonance in the K shell which exists at about 10 eV above the threshold [18,19]. Also there is no Cooper minimum at that energy. In other words, the known factors for increasing the nondipole effects mentioned above do not work here. The latest measurement and calculation [20] did not support the first observation and only a small effect was found in a broad energy region from the K shell ionization threshold up to about 70 eV above it.

In this paper we present the experimental and theoretical study of nondipole effects for the C K shell of CO molecules at photon energies from the ionization threshold up to about 80 eV above it. Two independent measurements have been performed at the Photon Factory in Tsukuba, Japan, and at the Advanced Light Source (ALS) in Berkeley, USA. In the only previously published report for CO [21] the nondipole effect was rather strong, especially at the threshold. Our results do not support that observation.

II. EXPERIMENTAL METHODS

At photon energies below 1 keV the following formula can be used to describe photoelectron angular distributions for 100% linearly polarized radiation [5]:

$$\frac{d\sigma}{d\Omega} = \frac{\sigma}{4\pi}\left[1 + \frac{\beta}{2}(3\cos^2\theta - 1) + (\delta + \gamma\cos^2\theta)\sin\theta\cos\phi \right].$$

$$(1)$$

Here β is the dipole angular asymmetry parameter, γ and δ are the first-order nondipole angular-distribution parameters, θ is the angle between the photon polarization vector $\mathbf{e}$ and the photoelectron momentum $\mathbf{p}$ and ϕ is the angle between the photon momentum $\mathbf{k}$ and the projection of $\mathbf{p}$ on the plane containing $\mathbf{k}$ and the vector $\mathbf{e} \times \mathbf{k}$. The dependence of Eq. (1) on the angle ϕ is the characteristic feature of the nondipole corrections. Equation (1) is equally applied to atoms and randomly oriented molecules.

A. Photon Factory measurements

The measurements have been performed at an undulator beamline BL-2C of the Photon Factory, which provides nearly 100% linearly polarized photons in the 250–1500 eV energy range [22]. We measure all the photoelectrons at one time by a coincidence velocity imaging apparatus and determine simultaneously the dipole β and the nondipole γ and δ parameters from photoelectron angular distributions in the

plane containing both the photon polarization vector $\mathbf{e}$ and the photon propagation vector $\mathbf{k}$. The apparatus is described in detail elsewhere [23]. Briefly, the photon beam was focused onto a supersonic molecular beam. The ions and electrons were guided by a uniform extraction electric field to opposite sides towards two area detectors with delay-line readout and detected in coincidence. The ions momenta were determined from the time of flight and the positions of impact on the area detector. The projections of the electron's momenta on the plane parallel to the electric field were determined from their positions of impact. The photon polarization vector $\mathbf{e}$ and the photon propagation vector $\mathbf{k}$ were in the plane parallel to the uniform electric field. Since photoelectron signals from the periphery of the molecular beam blur the photoelectron image, we have used coincident photoelectron signals with the molecular ions CO^{2+} and also with the fragment ion pairs C^+ and O^+ produced via Auger decay after the C $1s$ photoionization of CO. To wash out electron-ion vector correlations from the coincident photoelectron signals, the ion signals having velocity vector information are integrated over all the directions. This data processing gives the photoelectron angular distributions from randomly oriented CO molecules in the limited volume at the crossing point of the photon and molecular beams. We have confirmed that there are no differences between the photoelectron angular distributions from the coincident photoelectron signals with the fragment ion pairs of C^+ and O^+ and those from the coincident photoelectron signals with the molecular ions CO^{2+}.

Figure 1 shows the coordinate system of our experimental setup. The axis of the velocity imaging spectrometer of our apparatus was aligned to the y axis. Equation (1) is valid only for 100% linearly polarized photons and for the perfect alignment. Here, to take possible misalignment effects into account, a tilt angle ψ of the photon polarization vector $\mathbf{e}$ with respect to the x-z plane is introduced. The photoelectron angular distribution for this case has been derived by Shaw *et al.* [24]:

$$\frac{d\sigma}{d\Omega}(P,\psi) = \frac{\sigma}{4\pi}\left\{ \left[1 + \frac{\beta}{8}(1 + 3P\cos 2\psi)(3\cos^2\theta - 1) \right] \right.$$

$$+ \left[\delta + \gamma\cos^2\theta + \frac{\gamma}{8}(P\cos 2\psi - 1) \right.$$

$$\times (5\cos^2\theta - 1) \right]\sin\theta\cos\phi$$

$$+ \left[\frac{3\beta}{8}(P\cos 2\psi - 1) \right]\sin^2\theta\cos 2\phi$$

$$+ \left. \left[\frac{\gamma}{8}(P\cos 2\psi - 1) \right]\sin^3\theta\cos 3\phi \right\}, \quad (2)$$

where P is the degree of linear polarization. In the present case $\phi = 0$ or π, since the photoelectron angular distributions are measured as intensities concentrated around the circumference of a ring image, which correspond to the photoelectrons emitted in the x-z plane. As a first step we have measured Ne $1s$ photoelectron angular distributions to evaluate
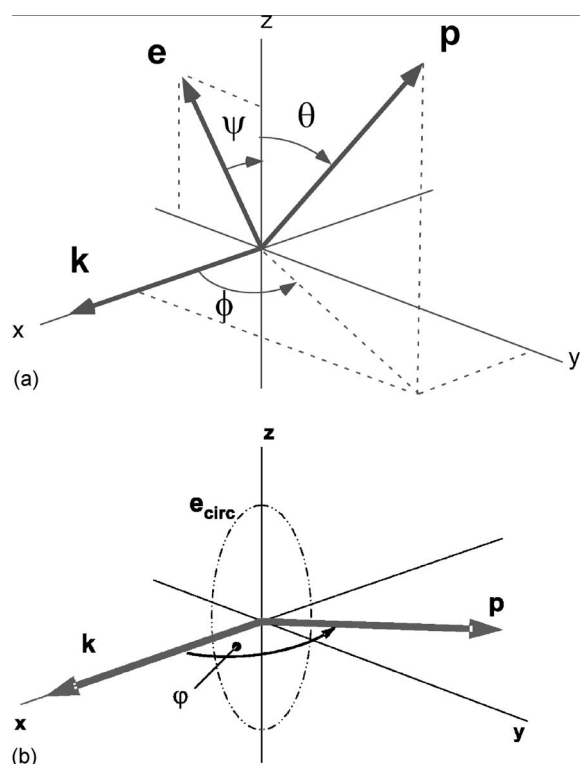
FIG. 1. The coordinate system of the two experimental setups. (a) The symmetry axis of the velocity imaging apparatus is aligned to the y axis. (b) For the case of circularly polarized light, the photoelectron angular distribution is only dependent on the angle φ between the photon propagation **k** and the direction of emission of the photoelectron **p**.

the polarization property of the photon beam. The dipole parameter β for the $1s$ shell is 2 by nonrelativistic theories [5,6]. Furthermore the relativistic model by Krässig *et al.* [25] gives $\beta > 1.98$, being consistent with their experimental results on Kr $1s$ shells for electron energies up to 2000 eV. Therefore, Eq. (2) with $\beta=2$ has been used to extract the nondipole parameters δ and γ and the polarization parameter $P \cos 2\psi$ from the measured angular distributions for Ne $1s$ shells by a least-squares fitting routine. The results are $\delta =-0.04\pm0.05$, $\gamma=-0.1\pm0.1$, and $P \cos 2\psi=0.98\pm0.01$ at a photon energy 900.3 eV (electron energy 30 eV). These results on the nondipole parameters for Ne are consistent with the nonrelativistic theoretical results, $\delta=0$ and $\gamma=-0.038$, by Bechler and Pratt [6].

A typical example of C $1s$ photoelectron angular distributions of CO molecules at a photon energy 325.9 eV (electron energy 30 eV) is shown in Fig. 2. Equation (2) with the substitution of $P \cos 2\psi=0.98\pm0.01$ has been used to extract the dipole and nondipole parameters from the angular distributions. For the test of our experimental system, we have measured the angular distribution of Ne $1s$ photoelectrons having the same energy as C $1s$ photoelectrons of CO at every stage in the course of the measurements of such photon energy dependence. And we have confirmed the similar results for the nondipole parameters and polarization parameters with the above-mentioned values for Ne over the entire electron energy range.
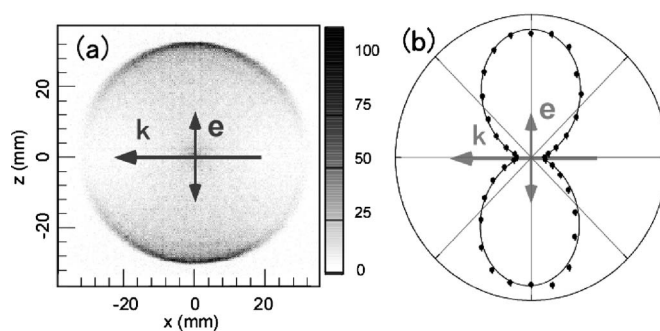

FIG. 2. The CO C $1s$ photoelectron image (a) and its angular distribution (b). The data were obtained at the photon energy 325.9 eV by the coincidence of C $1s$ photoelectrons with the fragment ion pairs C^+ and O^+ (see text). The bar coding shows the relative intensity of photoelectrons. To make the polar plot, the photoelectron intensities are integrated over the angles $\Delta\theta=5°$ and $\Delta\phi=20°$. Full circles, experimental data; and solid curve, fitted curve of Eq. (2).

B. ALS-COLTRIMS collaboration

Furthermore, several sets of measurements in the region of the carbon K threshold of the carbon monoxide were performed using the well-established COLTRIMS-technique [26,27] at a beamline 4.0.2 of the Advanced Light Source at the Lawrence Berkeley National Laboratory. The same endstation has been used to measure electron angular distributions from fixed in space CO, N_2, and C_2H_2 [28–31]. A supersonic gas jet is crossed with a circularly polarized photon beam thus creating a well-defined target region. Homogeneous electric and magnetic fields guide the photo fragments to two position and time sensitive detectors [32] as shown in Fig. 3. By measuring the time of flight and the position of impact of the electrons and ions that were created in the photo reaction, the vector momentum of each particle is obtained [33]. The spectrometer's fields and dimensions were chosen such that ions with a kinetic energy of 10 eV from the break-up of the carbon monoxide molecule and all photoelectrons are detected with a solid angle of 4π. A triple-coincident measurement of two ions and one electron was performed in order to identify the break-up channel of the
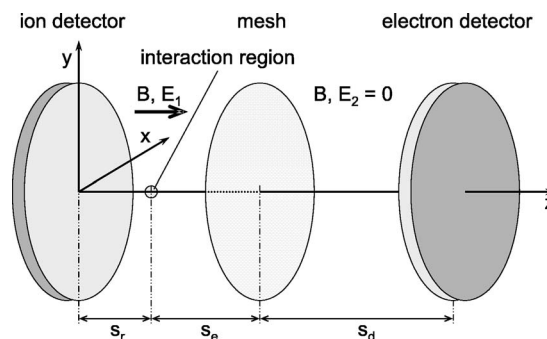

FIG. 3. A COLTRIMS-spectrometer employing McLaren-time focusing on the electron arm ($s_d=2s_e$) using a drifttube (right side). The circularly polarized light propagates along the x axis, its polarization plane lies within the y,z plane, and the direction of the supersonic jet coincides with the orientation of the y axis.

molecule and suppress events originating from reactions with background gas. Being the dominant channel close to the C K threshold, only events of photoionization leading to a break-up into two singly charged ions (C^+ and O^+) are considered in the offline analysis. From the momentum of the measured electrons the photoelectron is identified due to its kinetic energy, and its angular distribution of emission in the laboratory frame is acquired. The angular distribution for randomly oriented molecules is obtained by disregarding the information on the momentum of the measured photoions during offline analysis. For circularly polarized light the propagation direction of the photons is an axis of a rotational symmetry. Therefore, the angular distribution of the emitted photoelectrons is dependent only on the cosine of the angle φ between the electron momentum and the light propagation [see Fig. 1(b)], thus leading to [24]:

$$\frac{d\sigma}{d\Omega} = \frac{\sigma}{4\pi}\left[1 + \left(\frac{\beta}{4}\right) + \left(\delta + \frac{\gamma}{2}\right)\cos\varphi - \frac{3\beta}{4}\cos^2\varphi \right.$$
$$\left. - \frac{\gamma}{2}\cos^3\varphi \right]. \tag{3}$$

As the complete three-dimensional momentum space of the photoelectron is measured in the experiment, that rotational symmetry is used to avoid systematic errors and increase statistics: the angular distribution of photoelectrons is the same for any plane containing the propagation direction of the photons. Therefore, by integrating over all those planes in the offline analysis, the statistical error and possible systematic errors are reduced. By fitting Eq. (3) to the experimental angular distribution, the anisotropy and asymmetry parameters β, γ, and δ are obtained.

The measurement presented in this paper was carried out in 2002. Further measurements, that were done later on, support its results. The measurement was performed by scanning the photon energy from the threshold (296 eV) to 30 eV above it. With a second setup the experiment was done for fixed photon energies close to threshold. From the scattering of resulting asymmetry parameters it seems that systematic errors exceed the statistical errors in our measurement which is incorporated in the figures by increasing the statistical error bars by a factor of 2, leading to an estimated error of 0.2 for γ and 0.04 for δ. Therefore, in order to allow the reader to evaluate the overall validity of the experimental data, one of the measured angular distributions at a photon energy of $h\nu = 299.3$ eV is plotted together with the fitting curve in Fig. 4 (left). On the right side of that figure the angular distribution for the case of $\zeta = 1.3$ is plotted, in order to give an impression of how an angular distribution with nondipole contributions of the magnitude reported by Lindle *et al.* [21] is shaped.

III. THEORY

Our calculations in this paper are restricted by the Hartree-Fock (HF) approximation though we have the possibility to include many-electron correlations in the random phase approximation (RPA) as it was described in [34,35]. This is because the intrashell RPA correlations are usually
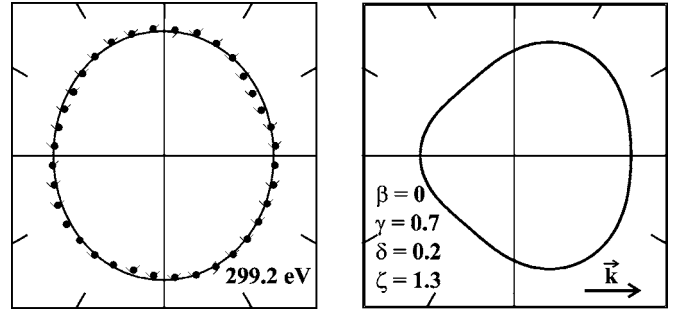

FIG. 4. Left. Measured CO-K photoelectron angular distribution for $h\nu = 299.2$ eV in a plane perpendicular to the polarization plane of the circularly polarized photons. The statistical error bars are smaller than the dot size of each data point. The line corresponds to a fit employing Eq. (3). Right: an example of an angular distribution with $\zeta = 1.3$.

small for two-electron subshells, and, in particular, for K shells of light atoms and molecules. As to the intershell correlations, they are giving a substantial contribution in the case of K shells of N_2 molecules due to a very small energy difference (about 0.1 eV) between the $1\sigma_g$ and $1\sigma_u$ shells, and due to existence of the σ^* shape resonance in the $1\sigma_g$ shell [35]. The C K shell of the CO molecule is separated in energy by about 200 eV from both the O K shell and the valence shells. Due to that the intershell RPA correlations for the C K shell of CO are negligible, too. We checked it numerically using our RPA program and found that the contribution of both intra- and intershell RPA correlations does not exceed 2%. The other kind of many-electron correlations describing the relaxation of the molecular wave functions after the creation of a deep hole in the K shell (which are beyond the RPA approximation) are really important, and they are taken into account by using the relaxed core HF approximation described below.

The Hartree-Fock ground state wave functions of a diatomic molecule are the solutions of the system of self-consistent equations

$$\left[-\frac{\nabla^2}{2} - \frac{Z_1}{r_1} - \frac{Z_2}{r_2} + \sum_{j=1}^{n} a_{ij}J_{jj}(\mathbf{r}) \right]\varphi_i(\mathbf{r}) - \sum_{j=1}^{n} b_{ij}J_{ij}(\mathbf{r})\varphi_j(\mathbf{r})$$

$$= \varepsilon_i\varphi_i(\mathbf{r}) + \sum_{j=1}^{n} \varepsilon_{ij}\varphi_j(\mathbf{r}), \tag{3'}$$

where n is the number of occupied orbitals, $i \leq n$, ε_i is the energy of the orbital, and $J_{ij}(\mathbf{r})$ are the Coulomb integrals defined as

$$J_{ij}(\mathbf{r}) \equiv J_{ij}(\varphi_i(\mathbf{r}), \varphi_j(\mathbf{r})) = \int \varphi_i(\mathbf{r}')|\mathbf{r} - \mathbf{r}'|^{-1}\varphi_j^*(\mathbf{r}')d\mathbf{r}'. \tag{4}$$

They describe the direct interaction when $i = j$ and the exchange interaction when $i \neq j$. The values of off-diagonal energy parameters ε_{ij} are determined from the orthogonalization condition

$$\int \varphi_i^*(\mathbf{r})\varphi_j(\mathbf{r})d\mathbf{r} = 0. \qquad (5)$$

In the case of a closed shell molecule the parameters of Eq. (1) are

$$a_{ij} = 2, \quad b_{ij} = 1; \quad \varepsilon_{ij} = 0. \qquad (6)$$

For an excited state wave function φ_f in the field of a singly charged ion, the equation in a frozen core HF approximation (FCHF) is similar to (3′)

$$\left[-\frac{\nabla^2}{2} - \frac{Z_1}{r_1} - \frac{Z_2}{r_2} + \sum_{j=1}^n a_{fj}J_{jj}(\mathbf{r}) \right]\varphi_f(\mathbf{r}) - \sum_{j=1}^n b_{fj}J_{fj}(\mathbf{r})\varphi_j(\mathbf{r})$$

$$= \varepsilon_f\varphi_f(\mathbf{r}) + \sum_{j=1}^n \varepsilon_{fj}\varphi_j(\mathbf{r}), \qquad (7)$$

where $f > n$,

$$a_{fj} = 2, \quad b_{fj} = 1, \quad j \neq i';$$

$$a_{fi'} = 1, \quad b_{fi'} = -1. \qquad (8)$$

Here the index i' corresponds to the ionized shell, and the off-diagonal energy parameters provide the orthogonalization of the excited state wave function to the ground state (core) wave functions,

$$\int \varphi_f^*(\mathbf{r})\varphi_i(\mathbf{r})d\mathbf{r} = 0. \qquad (9)$$

It is known that in the case of the ionization of K shells a core relaxation after ejection of one core electron plays an important role [36]. It is usually taken into account in the framework of the relaxed core HF (RCHF) approximation implying that the excited state wave functions satisfy Eq. (7) with the potential calculated with another set of wave functions. Namely, the new set of the self-consistent bound state wave functions of the molecular ion is calculated with one electron eliminated from the (two-electron) i' shell. It is achieved by solving Eq. (3′) with the coefficients given below

$$a_{i'i'} = b_{i'i'} = 0; \quad a_{ii'} = 1, \quad b_{ii'} = 0.5, \quad i \neq i';$$

$$a_{i'j} = 2, \quad b_{i'j} = 1, \quad j \neq i'; \quad a_{ij} = 2, \quad b_{ij} = 1, \quad i \neq i'. \qquad (10)$$

Here the first line means that the HF interaction is absent in the one-electron ionized shell, and the HF interaction of the ionized shell with all others becomes two times smaller. The second line shows that the other parts of the HF interaction are not changed. The parameters $\varepsilon_{i'j} \neq 0$ and should be calculated to fulfill (5).

Usually the RCHF model overestimates the influence of the relaxation effects for K shells [36]. Therefore we are using here the fractional charge RCHF model which corresponds to some intermediate value of the charge of the hole state. Originally the idea of using a fractional charge (equal to 0.5) was proposed by Slater in his transition state approxi-

mation [37]. In our case we calculate the relaxed core wave functions $\varphi_f^R(r)$ as solutions of Eq. (1) with the coefficients lying between those given by Eqs. (4) and (8). Namely, the coefficients are expressed through the fractional parameter $z_e(0 < z_e < 1)$ by the equations

$$a_{i'i'} = 2(1 - z_e), \quad b_{i'i'} = 1 - z_e;$$

$$a_{ii'} = 2 - z_e, \quad b_{ii'} = 0.5(2 - z_e), \quad i \neq i';$$

$$a_{i'j} = 2, \quad b_{i'j} = 1, \quad j \neq i'. \qquad (11)$$

The FCHF model corresponds to $z_e = 0$, while the standard RCHF model corresponds to $z_e = 1$. The charge z_e is considered as a free parameter determined from the condition to better reproduces the experimental data. We accepted in this paper $z_e = 0.7$ which reproduce slightly better the position of the σ^* shape resonance than the charge $z_e = 0.5$ used in our previous calculation for the C K shell of CO [38].

For the angular-distribution calculations we define the photoelectron wave function $\psi_p^{(-)}(\vec{r})$ with the incoming-wave boundary condition by the equation

$$\psi_p^{(-)}(\vec{r}) = \sum_{l,m} i^l e^{-i\delta_{lm}} f_{\varepsilon lm}(\vec{r}) Y_{lm}^*(\Omega_p), \qquad (12)$$

where Ω_p are the spherical angles of the photoelectron momentum $\mathbf{p}$, $\varepsilon = p^2/2$ is the photoelectron energy, and δ_{lm} is its phase shift. The parameter β in Eqs. (1) and (2) is defined as before [38];

$$\beta = \frac{\sqrt{30}}{B} \sum_{l,l'} (i)^{l'-l}\sqrt{[l,l']}\begin{pmatrix} l & l' & 2 \\ 0 & 0 & 0 \end{pmatrix} \sum_{m,m'} \exp[i(\delta_{lm} - \delta_{l'm'})]$$

$$\times d_{lm}d_{l'm'}^*\begin{pmatrix} l & l' & 2 \\ m & -m' & m'-m \end{pmatrix}\begin{pmatrix} 1 & 1 & 2 \\ m & -m' & m'-m \end{pmatrix}, \qquad (13)$$

where $[l] \equiv (2l+1)$, d_{lm} is the dipole matrix element

$$d_{lm} = \sqrt{\frac{4\pi}{3}}\langle f_{\varepsilon lm}|rY_{1m}(\Omega_r)|i\rangle, \qquad (14)$$

with Ω_γ being the spherical angles of the photon polarization vector $\mathbf{e}$, $|i\rangle$ is the initial state of electron, and $B = \sum_{l,m} d_{lm}^2$. The nondipole parameters γ and δ in Eqs. (1) and (2) are expressed through the values

$$F_J = -c_J k \frac{6\sqrt{6}}{B}\begin{pmatrix} 1 & 2 & J \\ 0 & 1 & -1 \end{pmatrix} \sum_{l,l'} (i)^{l'-l}[J,l,l']\begin{pmatrix} J & l & l' \\ 0 & 0 & 0 \end{pmatrix}$$

$$\times \sum_{m,m'} \exp[i(\delta_{lm} - \delta_{l'm'})]\begin{pmatrix} J & l & l' \\ m'-m & m & -m' \end{pmatrix}$$

$$\times \begin{pmatrix} 1 & 2 & J \\ m & -m' & m'-m \end{pmatrix}\mathrm{Re}(d_{lm}q_{l'm'}^*), \qquad (15)$$

$J = 1, 3$; $c_1 = 1$, $c_3 = \sqrt{7/8}$;
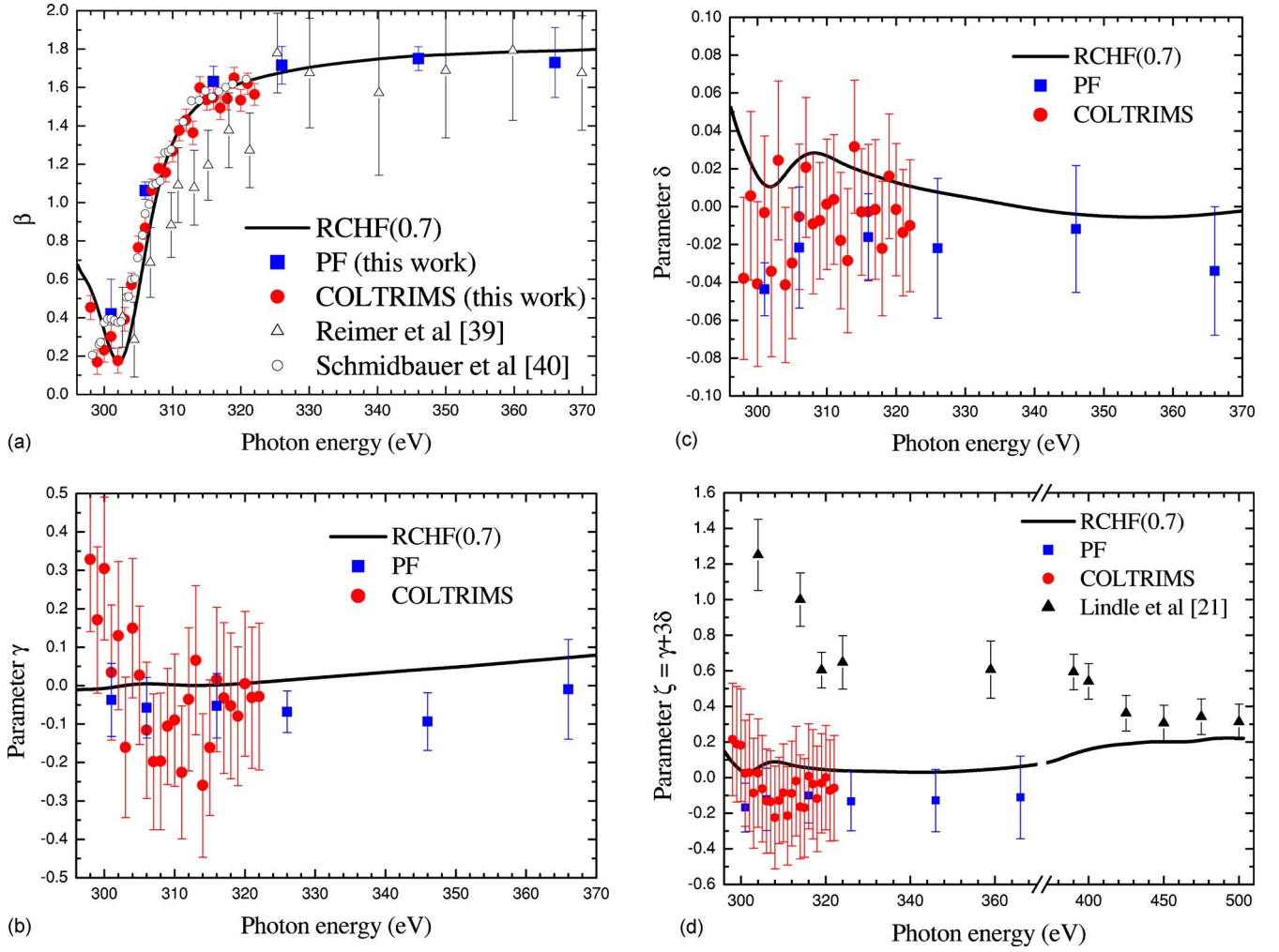
FIG. 5. (Color online) The angular asymmetry parameter β (a), and the nondipole parameters γ (b), δ (c), and ζ (d) for the C K shell of CO molecules. Filled circles with error bars, the COLTRIMS experiment; filled squares, the PF experiment; solid curves, RCHF(0.7) calculation. The experimental data of other authors are explained in the figures.

$$G_1 = k\frac{6\sqrt{3}}{B}\sum_{l,m}\sum_{l',m'} (i)^{l'-l}\exp[i(\delta_{lm} - \delta_{l'm'})]\sqrt{[l,l']}\begin{pmatrix} l & l' & 1 \\ 0 & 0 & 0 \end{pmatrix}$$

$$\times \begin{pmatrix} l & l' & 1 \\ m & -m' & m'-m \end{pmatrix}$$

$$\times \begin{pmatrix} 1 & 1 & 1 \\ m'-m & m & -m' \end{pmatrix}\text{Im}(d_{lm}M^*_{lm'}), \qquad (16)$$

by the relations

$$\delta = F_1 - F_3 + G_1, \quad \gamma = 5F_3. \qquad (17)$$

In Eqs. (15) and (16) k is the photon momentum, the electric quadrupole q_{lm}, and the magnetic dipole M_{lm} matrix elements are defined as

$$q_{lm} = \frac{\sqrt{2\pi}}{15}\langle f_{\varepsilon lm}|r^2 Y_{2m}(\Omega_r)|i\rangle, \quad M_{lm} = \frac{1}{\sqrt{2}}\langle f_{\varepsilon lm}|L_m|i\rangle,$$

$$(18)$$

and L_m are spherical projections of the angular momentum operator. The contribution of the partial waves up to $l=7$ has

been taken into account in Eqs. (12)–(18) in our numerical calculations.

IV. RESULTS

The results of our studies for the dipole and nondipole angular asymmetry parameters are presented in Fig. 5. Figure 5(a) demonstrates the dipole angular asymmetry parameter β. The two experiments reported here agree quite well with each other and with the RCHF (0.7) calculation. The earlier measurements of Reimer *et al.* [39] have rather large error bars and differ somewhat from our data, while there is a perfect agreement with the more recent data of Schmidbauer *et al.* [40].

Figures 5(b) and 5(c) show the nondipole parameters γ and δ. Both experiments agree within the error bars with a value of zero for the two asymmetry parameters in the examined region of the photon energy. The deviations from zero, that are observed by the RCHF (0.7) theory, are smaller than the experimental accuracy. From the experimental side lower and upper bounds for the values of the nondipole pa-
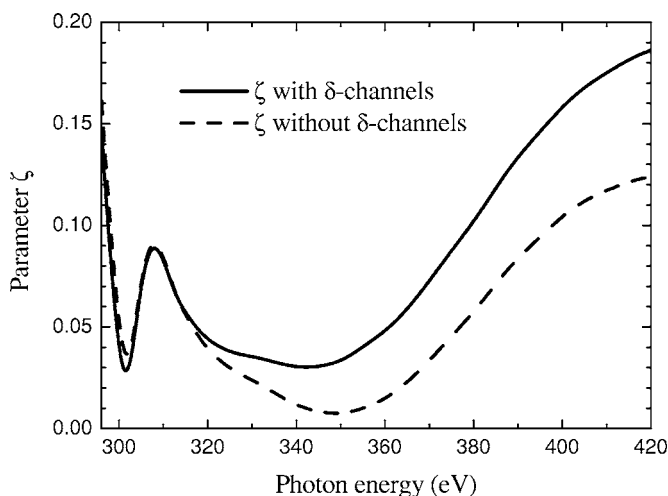
FIG. 6. The results of RCHF(0.7) calculations for the ζ parameter of the C K shell with (solid line) and without (dashed line) inclusion of the contribution of the δ quadrupole channels.

rameters can be given as $-0.3 < \gamma < 0.3$ and $-0.05 < \delta < 0.05$.

Finally, Fig. 5(d) shows the parameter ζ. Contrary to the earlier measurements of Lindle *et al.* [21] both PF and COLTRIMS experiments give close to zero values near the threshold in full agreement with the RCHF(0.7) theory. According to Ref. [16] there is a large contribution of the δ quadrupole channels to the maximum of the ζ parameter at 460 eV photon energy in N_2 molecules. We demonstrate in Fig. 6 the results of our calculations of the ζ parameter for CO molecules with and without an inclusion of the δ channels. Their contribution is close to zero at the threshold and is slowly increasing with photon energy remaining relatively small at all energies studied.

Since in [21] the ζ parameter has been measured to higher energies than in the present experiments, we calculated the ζ parameter to the same energies [see Fig. 5(d)]. Above 420 eV photon energy the values measured in [21] become rather small and agree quite well with our theory.

V. SUMMARY

Initiated by previous experiments [16,17,21], a new study of the nondipole effects in the angular distribution of photo-

electrons from the C K shell of CO molecules has been undertaken. Two independent measurements in different laboratories have been performed for both dipole and nondipole angular asymmetry parameters. The results of these measurements agree quite well with each other and demonstrate that all three nondipole parameters, γ, δ, and ζ are small in the photon energy region from ionization threshold to about 70 eV above it. This is in contradiction with the earlier measurement [21] where the parameter ζ near the ionization threshold was found to exceed 1 in magnitude. Simultaneously the calculation of all the parameters in the relaxed core HF approximation with the fractional charge equal to 0.7 has been performed. The theoretical values of all nondipole parameters are also small, and usually coincide with our experimental data within the error bars. A good agreement between the RCHF(0.7) theory and two experiments can be considered as a proof of reliability of the results. Together with the analogous results for the N_2 molecule obtained recently [20] our study demonstrates that the nondipole effects in the vicinity of the C K shell ionization threshold of CO molecules do not play a dramatic role in photoionization and in many cases can be disregarded. For the β parameter there is a good agreement between theory and both experiments, as well as with the earlier measurements.

[1] M. O. Krause, Phys. Rev. **177**, 151 (1969).
[2] F. Wuilleumier and M. O. Krause, Phys. Rev. A **10**, 242 (1974).
[3] O. Hemmers, R. Guillemin, and D. W. Lindle, Radiat. Phys. Chem. **70**, 123 (2004).
[4] M. Ya. Amusia, P. U. Arifov, A. S. Baltenkov, A. A. Grinberg, and S. G. Shapiro, Phys. Lett. **47A**, 66 (1974).
[5] J. W. Cooper, Phys. Rev. A **42**, R6942 (1990); **47**, 1841 (1993).
[6] A. Bechler and R. H. Pratt, Phys. Rev. A **39**, 1774 (1989); **42**, 6400 (1990).
[7] A. Derevianko, W. R. Johnson, and K. T. Cheng, At. Data

Nucl. Data Tables **73**, 153 (1999).
[8] V. I. Nefedov, V. G. Yarzhemsky, I. S. Nefedova, and M. B. Trzhaskovskaya, J. Electron Spectrosc. Relat. Phenom. **113**, 91 (2000).
[9] N. L. S. Martin, D. B. Thompson, R. P. Bauman, C. D. Caldwell, M. O. Krause, S. P. Frigo, and M. Wilson, Phys. Rev. Lett. **81**, 1199 (1998).
[10] V. K. Dolmatov and S. T. Manson, Phys. Rev. Lett. **83**, 939 (1999).
[11] W. R. Johnson and K. T. Cheng, Phys. Rev. A **63**, 022504 (2001).
[12] N. A. Cherepkov and S. K. Semenov, J. Phys. B **34**, L495

(2001).

[13] N. A. Cherepkov, S. K. Semenov, M. Drescher, and U. Heinzmann, J. Phys. B **36**, 3063 (2003).

[14] S. Ricz, R. Sankari, A. Kövér, M. Jurvansuu, D. Varga, J. Nikkinen, T. Ricsoka, H. Aksela, and S. Aksela, Phys. Rev. A **67**, 012712 (2003).

[15] O. Hemmers *et al.*, Phys. Rev. Lett. **91**, 053002 (2003).

[16] O. Hemmers, H. Wang, P. Focke, I. A. Sellin, D. W. Lindle, J. C. Arce, J. A. Sheehy, and P. W. Langhoff, Phys. Rev. Lett. **87**, 273003 (2001).

[17] P. W. Langhoff, J. C. Arce, J. A. Sheehy, O. Hemmers, H. Wang, P. Focke, I. A. Sellin, and D. W. Lindle, J. Electron Spectrosc. Relat. Phenom. **114–116**, 23 (2001).

[18] J. L. Dehmer and D. Dill, Phys. Rev. Lett. **35**, 213 (1975).

[19] E. Shigemasa, K. Ueda, Y. Sato, T. Sasaki, and A. Yagishita, Phys. Rev. A **45**, 2915 (1992).

[20] K. Hosaka, J. Adachi, A. V. Golovin, M. Takahashi, T. Teramoto, N. Watanabe, A. Yagishita, S. K. Semenov, and N. A. Cherepkov, J. Phys. B **39**, L25 (2006).

[21] D. W. Lindle, O. A. Hemmers, H. Wang, P. Focke, I. A. Sellin, J. D. Mills, J. A. Sheehy, and P. W. Langhoff, *XIX ICPEAC, Invited Papers, p. XX.*

[22] M. Watanabe, A. Toyoshima, Y. Azuma, T. Hayaishi, Y. Yan, and A. Yagishita, Proc. SPIE **3150**, 58 (1998); M. Watanabe, A. Toyoshima, J. Adachi, and A. Yagishita, Nucl. Instrum. Methods Phys. Res. A **467–468**, 512 (2001).

[23] K. Hosaka, J. Adachi, A. V. Golovin, M. Takahashi, N. Watanabe, and A. Yagishita, Jpn. J. Appl. Phys. (to be published).

[24] P. S. Shaw, U. Arp, and S. H. Southworth, Phys. Rev. A **54**, 1463 (1996).

[25] B. Krässig, J.-C. Bilheux, R. W. Dunford, D. S. Gemmell, S. Hasegawa, E. P. Kanter, S. H. Southworth, L. Young, L. A. LaJohn, and R. H. Pratt, Phys. Rev. A **67**, 022707 (2003).

[26] R. Dörner, V. Mergel, O. Jagutzki, L. Spielberger, J. Ullrich, R. Moshammer, and H. Schmidt-Böcking, Phys. Rep. **330**, 96 (2000).

[27] J. Ullrich, R. Moshammer, A. Dorn, R. Dörner, L. Ph. H. Schmidt, and H. Schmidt-Böcking, Rep. Prog. Phys. **66**, 1463 (2003).

[28] A. Landers, Th. Weber, I. Ali, A. Cassimi, M. Hattass, O. Jagutzki, A. Nauert, T. Osipov, A. Staudte, M. H. Prior, H. Schmidt-Böcking, C. L. Cocke, and R. Dörner, Phys. Rev. Lett. **87**, 013002 (2001).

[29] T. Jahnke, Th. Weber, A. L. Landers, A. Knapp, S. Schössler, J. Nickles, S. Kammer, O. Jagutzki, L. Schmidt, A. Czasch, T. Osipov, E. Arenholz, A. T. Young, R. Diez Muino, D. Rolles, F. J. Garcia de Abajo, C. S. Fadley, M. A. Van Hove, S. K. Semenov, N. A. Cherepkov, J. Rösch, M. H. Prior, H. Schmidt-Böcking, C. L. Cocke, and R. Dörner, Phys. Rev. Lett. **88**, 073002 (2002).

[30] T. Jahnke, L. Foucar, J. Titze, R. Wallauer, T. Osipov, E. P. Benis, A. Alnaser, O. Jagutzki, W. Arnold, S. K. Semenov, N. A. Cherepkov, L. Ph. H. Schmidt, A. Czasch, A. Staudte, M. Schöffler, C. L. Cocke, M. H. Prior, H. Schmidt-Böcking, and R. Dörner, Phys. Rev. Lett. **93**, 083002 (2004).

[31] T. Osipov, C. L. Cocke, M. H. Prior, A. Landers, T. Weber, O. Jagutzki, L. Schmidt, H. Schmidt-Böcking, and R. Dörner, Phys. Rev. Lett. **90**, 233002 (2003).

[32] http://www.roentdek. com.

[33] T. Jahnke, Th. Weber, T. Osipov, A. L. Landers, O. Jagutzki, L. Ph. H. Schmidt, C. L. Cocke, M. H. Prior, H. Schmidt-Böcking, and R. Dörner, J. Electron Spectrosc. Relat. Phenom. **73**, 229 (2004).

[34] S. K. Semenov and N. A. Cherepkov, Chem. Phys. Lett. **291**, 375 (1998).

[35] S. K. Semenov and N. A. Cherepkov, Phys. Rev. A **66**, 022708 (2002).

[36] D. L. Lynch and V. McKoy, Phys. Rev. A **30**, R1561 (1984).

[37] J. C. Slater, *The Self-Consistent Field for Molecules and Solids: Quantum Theory of Molecules and Solids* (McGraw-Hill, New York, 1974), Vol. 4.

[38] S. K. Semenov, N. A. Cherepkov, T. Jahnke, and R. Dörner, J. Phys. B **37**, 1331 (2004).

[39] A. Reimer, J. Schirmer, J. Feldhaus, A. M. Bradshaw, U. Becker, H. G. Kerkhoff, B. Langer, D. Szostak, R. Wehlitz, and W. Braun, Phys. Rev. Lett. **57**, 1707 (1986).

[40] M. Schmidbauer, A. L. D. Kilcoyne, H. M. Köppe, J. Feldhaus, and A. M. Bradshaw, Chem. Phys. Lett. **199**, 119 (1992).